The American Journal of Human Genetics, Volume *102*

Supplemental Data

Functional Dysregulation of CDC42

Causes Diverse Developmental Phenotypes

Simone Martinelli, Oliver H.F. Krumbach, Francesca Pantaleoni, Simona Coppola, Ehsan Amin, Luca Pannone, Kazem Nouri, Luciapia Farina, Radovan Dvorsky, Francesca Lepri, Marcel Buchholzer, Raphael Konopatzki, Laurence Walsh, Katelyn Payne, Mary Ella Pierpont, Samantha Schrier Vergano, Katherine G. Langley, Douglas Larsen, Kelly D. Farwell, Sha Tang, Cameron Mroske, Ivan Gallotta, Elia Di Schiavi, Matteo della Monica, Licia Lugli, Cesare Rossi, Marco Seri, Guido Cocchi, Lindsay Henderson, Berivan Baskin, Mariëlle Alders, Roberto Mendoza-Londono, Lucie Dupuis, Deborah A. Nickerson, Jessica X. Chong, The University of Washington Center for Mendelian Genomics, Naomi Meeks, Kathleen Brown, Tahnee Causey, Megan T. Cho, Stephanie Demuth, Maria Cristina Digilio, Bruce D. Gelb, Michael J. Bamshad, Martin Zenker, Mohammad Reza Ahmadian, Raoul C. Hennekam, Marco Tartaglia, and Ghayda M. Mirzaa

SUPPLEMENTAL DATA

TABLE OF CONTENTS

Supplemental Clinical Data.

Figure S1. Pedigree of family 30153 showing transmission of the CDC42 variant and its co-segregation with the trait.

Figure S2. Basal and GAP-stimulated GTPase activity of disease-causing CDC42 mutants.

Figure S3. Basal and GEF-catalyzed nucleotide exchange reactions of disease-causing CDC42 mutants.

Figure S4. Binding of disease-causing CDC42 mutants to diverse effectors.

Figure S5. *CDC42* mutations differentially impact polarized migration.

Figure S6. Amino acid sequence alignments of human CDC42 and the *C. elegans* ortholog.

Figure S7. Consequences of CDC-42 expression on vulval development in *C. elegans*.

Figure S8. Brain MRIs of *CDC42* mutation-positive individuals.

Table S1. WES data output of *CDC42* mutation-positive individuals.

Table S2. Interpretation of the identified *CDC42* variants according to ACMG criteria.

Table S3. Vulval phenotypes in nematodes expressing wild-type CDC-42 or the disease-associated mutants.

Table S4. Impact of *wsp-1*/*WASP* RNA-mediated interference on vulval phenotypes in *C. elegans*.

Table S5. Clinical features of *CDC42* mutation-positive individuals.

Table S6. Details of the facial features of *CDC42* mutation-positive individuals.

Table S7. Neuroimaging features of *CDC42* mutation-positive individuals.

SUPPLEMENTAL CLINICAL DATA

Subject 1 (LR16-483; p.Ile21Thr)

This African American male was born to healthy, non-consanguineous parents. He has a healthy older brother. He was born at 35 weeks of gestation and was hospitalized for three weeks because of feeding issues, poor suck, and respiratory difficulties. He was referred to Genetics at age 5 months due to three failed hearing screens and mild dysmorphic facial features including a prominent forehead, a high and narrow nasal bridge, broad nasal tip, apparent synophrys with prominent metopic sutures. At that time, he was noted to have some developmental delays. His head growth began to decrease starting at age 1 month. He underwent release of his tethered cord (just below L2) at age 16 months. He also has a history of equinus deformity of the left foot. He was diagnosed with unilateral renal agenesis following frequent urinary tract infections. He did not speak until almost age 2 years, requiring speech therapy through elementary school. He had inguinal hernia repair and urethral repair with orchidoplasty at age 6 years. He also has a diagnosis of attention-deficit hyperactivity disorder (ADHD) requiring medication. He had scoliosis and was followed by orthopedic surgery. He was evaluated by hematology and oncology specialists in 2017 following a complete blood count (CBC) that showed a total white blood cell (WBC) count of 1,900/mm^3 with an absolute neutrophil count (ANC) of 600/mm^3 and platelets of 143,000/mm^3. A recheck noted his total WBC count was up to 2.9 K/mm^3, his ANC was 900 and his platelets were 270. Brain MRI performed at 13 months was normal. Previous normal genetic tests included chromosomes, subtelomeric FISH, and SNP chromosomal microarray.

Subject 2 (LR14-224; p.Tyr23Cys)

This child's family consisted of healthy parents, two male children and one female child. The proband was 4 years of age at time of referral and presented with severe intellectual deficiency (ID), growth failure, autistic features, microcephaly, seizures, absent speech, and dysmorphic facial features including unilateral ptosis, up-turned nasal tip, short philtrum, and long neck. Developmentally, he gained head control at age 4 to 6 months, sat independently at 9 months, and walked at 24 months of age. He began having seizures at 5 months of age. He has been diagnosed with secondary generalized epilepsy with multiple seizure types. His seizures have been medically refractory. At his most recent visit at age 17 years, his seizures were relatively under good control with zonisamide and lacosamide. He remained nonverbal, but he can follow commands and answer questions by signing. Brain MRI performed at 1 years showed diffuse cerebral and cerebellar atrophy, mild cerebellar vermis hypoplasia, ventriculomegelay and thin corpus callosum. Extensive biochemical and genetic testing failed to identify an underlying disease etiology including chromosome analysis, subtelomeric FISH, CGH/SNP microarray, methylation testing for Angelman/Prader Willi syndrome and uniparental disomy, *MECP2*, *CDKL5*, *FOXG1*, *ARX* sequencing, a 90 gene X-linked intellectual disability gene panel, a 53-gene seizure panel, and a 101 nuclear mitochondrial gene panel, in addition to several biochemical tests, all of which were inconclusive.

Subject 3 (LR17-420; p.Tyr64Cys)

The proband is a 15-year-old female followed since birth by the Genetics service at the Hospital for the Sick Children. She is the only child of a 32-year-old mother of Filipino descent and a 60-year-old father of English descent. She was born at 41 weeks by spontaneous vaginal delivery after an uneventful pregnancy. Apgar scores were 5 at 1 minute and 7 at 5 minutes, respectively. Birth weight was 2.44 kg (–2 SD below the mean), length 50 cm (50^{th} centile) and occipito-frontal circumference (OFC) 32 cm (–2.2 SD below the mean). She had dysmorphic features including hypertelorism, low-set ears, upslanting palpebral fissures, medially-flared eyebrows and small chin,

in addition to distal arthrogryposis. She also had a two-vessel cord. She developed cyanosis and was admitted to the Neonatal Intensive Care Unit at birth. She was ventilated for 2 days. Echocardiogram showed ventricular septal defect (VSD), patent ductus arteriosus (PDA) and atrial septal defect (ASD). The ASD and VSD were repaired at age of 15 months, and the PDA closed spontaneously. Head ultrasound showed no major structural anomalies. She had feeding problems from birth that required nasogastric tube feeds. A G-tube was placed for severe gastro-esophageal reflux disease (GERD) at 4 months of age, and was required until the patient was 6 years old. She had persistent constipation that is still managed with PEG flakes. At age 8 months, ABR confirmed profound hearing loss on the right side and significant partial loss on the left side. At age 13 months, she was diagnosed with myxedema secondary to severe hypothyroidism, which has since been treated. Renal ultrasound showed mild bilateral pelviectasis. At age 3.5 years, the child underwent bilateral inguinal hernia repair. History is also remarkable for multiple allergies to medications and recurrent infections, including multiple viral and respiratory infections and bacteremia with low B-cell and T-cell counts, as well as low immunoglobulins. She has intermittent thrombocytopenia and neutropenia, asthma, and eczema. She has not experienced any significant infections since prophylactic amoxicillin was initiated at age 12 years. Examination of the limbs revealed limitations of the proximal interphalangeal (PIP) and distal interphalangeal (DIP) joints in both hands with left index finger being most severely affected. The fingers were also noted to be tapered and slender. In the lower limbs, the right 4th digit was noted to be proximally inserted. The range of movement of the large joints was within normal limits. She also had truncal hypotonia, with normal patellar reflexes.

The subject developed more significant camptodactyly over time. At the last examination, at age 15 years, her dysmorphic facial features had become more obvious. She had upslanting palpebral fissures, small and thin nose, flat philtrum, thin upper lip with downturned corners of the mouth, prominent glabella and small ears. From a developmental standpoint, she had global developmental delay. She walked with support at age 2.5 years. At 15 years of age, she could walk independently, but had an unstable wide-based gait and triped easily. She has remained without intelligible words, but learned to communicate with a private repertoire of gestures. She does not write or read, but used an I-pad with a Pro Logic II program for general communication primarily at school and at home, due to anxiety in other settings. She is partially toilet trained. With regards to other systems, fundus examination was grossly normal, although the optic nerves were noted to be somewhat pale with possible subtle nerve fiber layer loss. Abdominal ultrasound in the neonatal period showed a Superior Mesenteric Vein (SMV) directly anterior to the Superior Mesenteric Artery (SMA). She had a normal IGF1 of 147 μg/L at age 7 years. Spinal radiographs demonstrated subtle scoliosis measuring 14 degrees, and a 67 degree kyphosis measured between T5 and12.

Subject 4 (LR14-352; p.Arg66Gly)

This family consisted of the proband, parents and five older siblings. The proband was a 16-year-old male with a complex medical history characterized by multi-system involvement including intrauterine growth retardation, growth hormone deficiency, precocious puberty, and immunodeficiency (hypogammaglobulinemia associated with multiple infections). He received Intravenous Immunoglobulin (IVIG) in several forms with a reduction in the frequency of infections. The subject also has multiple vertebral anomalies, spinal fusion and kyphosis, widened central spinal canal, abnormal renal vascular system (4 renal arteries on the right and 3 renal arteries on the left), severe progressive hearing loss, hyperopia with anomalous optic nerves and thick corneas, annular pancreas, dysmorphic facial features (broad forehead, bilateral ptosis, a high, narrow nasal bridge with a broad nasal tip, wide mouth and widely spaced teeth), submucous cleft palate, syndactyly of the hands and feet (consists of 3-4 syndactyly of the left hand and 2-3 syndactyly of both feet), peg-like teeth (suggestive of ectodermal dysplasia), Legg-Calve-Perthes

disease of the right hip, multiple dysplastic skin moles, history of chronic loose bowel movements, chordee, learning disability, and developmental delay.

At the time of this report (18 year-old), the subject had undergone 39 surgeries including gastrostomy (G-) tube placement, annular pancreas repair, pericardial effusion that required pericardiectomy, cochlear implant placement, syndactyly and cleft palate repair, hemi-laminectomy at L1-L2 vertebral levels, bilateral decompression at L3-L4, bilateral proximal femoral and distal femoral extension osteotomies, and tibial de-rotation. He has intermittent treatment for hypertension, and has multiple joint contractures. Magnetic Resonance Imaging (MRI) of the brain showed abnormal signals in the periventricular white matter suggestive of dysmyelination. Renal computed tomography (CT) and angiography revealed multiple small renal arteries. Further testing revealed that Factor 13, Subunit A antigen levels were low. He underwent the following tests, which were inconclusive: karyotypes of blood and skin, telomeric FISH, array CGH, *TP63* sequence analysis, urine mucopolysaccharide (MPS) and oligosaccharide levels, and Factor 8 and Von Willebrand antigen levels.

Of his five siblings, one brother has pectus excavatum and a history of abnormal moles, another was born with a submucous cleft, and one sister had 3 pilonidal cysts, which were surgically-removed. The proband has several cousins who also presented with developmental problems, including two males with Asperger Syndrome and one male with pilonidal cysts (children of proband's 1st maternal uncle), one female with scoliosis (daughter of proband's 2nd maternal uncle), one female with an open fistula at the base of her neck (daughter of proband's maternal aunt), and one female who suffered sudden death at age 14 due to seizure (daughter of proband's paternal aunt).

Subject 5 (PCGC 1-04248; p.Arg66Gly)

This individual is a Caucasian-of-European-descent female infant who was born to healthy non-consanguineous parents. The mother was age 28.4 years and the father was 27.1 years at the time of delivery. This infant was born with aortic coarctation with stenosis of the left coronary artery ostium and bilateral pulmonary branch stenosis. Medical history is also remarkable for failure to thrive, mild developmental delays, and decreased hearing. This individual died around age 8 months due to cardiovascular complications, with otherwise limited medical data.

Subject 6 (ISS3MO; p.Arg68Gln)

This boy was born to healthy non-consanguineous parents. Mother was 35 years and father 40 years at the time of delivery. The child was born prematurely at 27 weeks of gestation. Birth weight was 965 grams (50^{th} percentile for gender and gestational age), length 32 cm (6^{th} percentile for gender and gestational age), and OFC 25 cm (–0.25 SD for gender and gestational age). He had a history of poor sucking and swallowing. His growth measurements on last assessment at age 4 years were 13 Kg ($<3^{rd}$ centile, –2.4 SD), length 93 cm ($<3^{rd}$ centile, –2.29 SD) and OFC 49 cm ($<3^{rd}$ percentile). He had several dysmorphic facial features including sparse hair with whorls, prominent forehead, epicanthal folds, wide nasal bridge, flared nostrils with a broad nasal tip, long philtrum, an under-developed midface, thick ears and a webbed appearance of the neck. He had sensorineural hearing loss, with a 50-70 DB threshold. Developmentally, he had cognitive deficits. His Griffiths developmental quotient was 70 at 24 months. He also had a history of hypertrophic cardiomyopathy, thrombocytopenia, elbow and arm contractures. He had a recurrent maculopapular cutaneous eruption, gastrointestinal bleeding episodes, recurrent fever, as well as polyserositis (pleural, pericardial effusion and ascites). He also had splenomegaly. His brain MRI showed mildly prominent periventricular white matter signal intensities (predominantly posteriorly), ventriculomegaly and increased extra-axial space. Previously performed genetic testes included an array CGH which revealed a paternally-inherited 716Kb deletion of 14q13.1, as well as sequencing

of the *PTPN11, SOS1, RAF1, KRAS, BRAF, MEK1, MEK2, HRAS, NRAS,* and *SHOC2* genes, which were all normal.

Subject 7 (ISS4BO; p.Arg68Gln)

This girl was born at term (at a gestational age of 39 weeks and two days) to healthy non-consanguineous parents. Birth weight was 3455 grams (0 SD), length 47 cm (25th centile) and OFC 36 cm (+1.5 SD). Apgar scores were 8, 9 at 1, 5 minutes, respectively She was 5 years-old at the time of the last clinical evaluation and growth measurements were the following: weight 15.5 Kg (3-10th centile), length 101 cm (3-10th centile), OFC 51 cm (+0.25 SD). Facial examination showed several dysmorphic facial features including spare hair and eyebrows, broad, prominent forehead, wide nasal bridge, long philtrum, underdeveloped mid-face, cubid's bow and low-set ears. A ventricular septal defect (VSD) was detected prenatally and confirmed at birth. Surgical correction was undertaken at the age of 3 years. She also had bilateral inguinal hernia that was treated surgically at the age of six months. She presented with early-onset thrombocytopenia, with a platelet count of 19,000-69,000/mmc, with occasional giant platelets identified by blood smear analysis, associated with macrocytic anemia. She also had sensorineural deafness with a 60-70 DB threshold. Developmentally, the child had global developmental delay. She could walk unassisted at age 30 months. However, language of the child continued to be non-verbal at last clinical evaluation. She had febrile seizures, with four reported seizure episodes. Brain MRI showed partial agenesis of the corpus callosum and sub-ependymal heterotopia.

Subject 8 (LR17-032; p.Cys81Phe)

The subject is a 4-year-old boy born to healthy, non-consanguineous parents. He has a healthy and developmentally-normal older brother. He was born at 38 weeks of gestation. Birth weight was 2.89 Kg (10-25th percentile), and length 45.7 cm (–2 SD). The child had a history of recurrent infections, gastroesophageal reflux disease, speech delays and microcephaly. He also has ptosis, strabismus, dysmorphic facial features (including wide palpebral fissures, up-turned nasal tip, flattened nasal bridge, thin upper lip, long philtrum, down turned corners of the mouth, low-set ears), and webbing of the penis. His growth had been consistently tracking below the 5th percentile. Vision and hearing were normal. Developmentally, he had speech delays, with velopharyngeal insufficiency for which a pharyngeal flap repair has been recommended. Otherwise, his cognitive development was assessed to be age-appropriate at age 4 years. Brain MRI showed prominent perivascular spaces throughout the deep white matter and basal ganglia, mild thinning of the corpus callosum and mega cisterna magna.

Subject 9 (LR10-046; p.Ser83Pro)

This boy was born to healthy non-consanguineous parents. He was conceived by In Vitro Fertilization (IVF). He had several complex medical issues. He was noted to have hydrocephalus with ventriculomegaly on early brain MRI scans and underwent ventriculoperitoneal (VP) shunt placement at 8 months of age. He had several dysmorphic facial features including a broad, prominent forehead, wide nasal bridge, long philtrum, cubid's bow, broad jaw, and widely-spaced teeth. Ventriculomegaly resolved after shunting. He also had congenital heart disease including total anomalous pulmonary venous return (TAPVR) and coarctation of the aorta status post-surgical correction. He was formally diagnosed with growth hormone deficiency, short stature and hypothyroidism. He was noted to have anhidrosis and easily became hyperthermic. Spinal imaging showed a tethered cord with the conus ending at L2-L3 level, as well as a syrinx extending from T2-L1. He had recurrent respiratory infections including several episodes of pneumonias, with no evidence of immunodeficiency. He also has recurrent asthma. Other medical issues include

strabismus that was surgically repaired, scoliosis, epilepsy, intellectual disability, and Autism Spectrum Disorder (ASD).

Subject 10 (LR16-056; p.Ser83Pro)

The proband is a 34-year-old male who was born to 34-year-old mother and 37-year-old father. Birth weight was 3270 grams (–0.5 SD) and length was 49.5 cm (~0 SD). He had several dysmorphic facial features that evolved over time including spare hair, prominent forehead, hypertelorism, bilateral ptosis, wide nasal bridge, flared nostrils, wide mouth with widely-spaced teeth. He had history of congenital lymphedema that has persisted throughout his life, a history of meningitis at age 4 months, and frequent episodes of cellulitis in lymphedematous legs. Recurrent infections subsided around adolescence. He had a history of myoclonic seizures during infancy and later in puberty. His growth measurements at age 34 years were the following: weight 70 Kg, and height 161 cm (–2.5 SD). He had mild developmental delays. He had good verbal language development but poor overall developmental functioning, and poor visual memory. Brain MRI at age 34 years showed ventriculomegaly and cerebellar tonsillar ectopia.

Subject 11 (LR15-338; p.Ala159Val)

This 7 year-old proband was the product of a 38-week gestation to 26-year-old G4, P0-1 mother. Pregnancy was complicated by a concern for a Dandy-Walker malformation on prenatal ultrasound and a single umbilical artery. Amniocentesis demonstrated a normal 46,XY karyotype. Apgar scores after birth were 9 and 9 at 1 and 5 minutes, respectively. His birthweight was 2.49 Kg (–2 SD), length 45 cm (–2 SD), and head circumference 31 cm (–3 SD). The diagnosis of a Dandy-Walker malformation was confirmed through a postnatal CT scan which also showed dysgenesis of the corpus callosum. Brain MRI was markedly abnormal and showed wide-spread white matter signal intensities, partial agenesis of the corpus callosum, and marked abnormalities of the cerebellum, brainstem and hippocampus. He had diffuse cerebellar foliar dysplasia with a large inferior cerebellar peduncle, small middle cerebellar peduncle, and stretched superior cerebellar peduncle. The cerebellar vermis was small and uprotated, consistent with a Dandy-Walker malformation. The thalami were small, along with the medulla and pons, with a cleft in the tectum. The hippocampus was unilaterally dysplastic as well. A renal ultrasound was also obtained and showed hydronephrosis. Physical examination at the time also demonstrated hypospadias, undescended testes, and a dilated left pupil on ocular exam. He was subsequently transferred to a nearby Children's Hospital for further evaluation and was discharged from the neonatal intensive care unit (NICU) there at 2 weeks of age. He followed with nephrology for asymmetric kidney size with poor corticomedullary differentiation and pelviectasis. He was also diagnosed with cerebral palsy and seizures. He followed up with ophthalmology for oculomotor nerve palsy and required glasses for strabismus. Developmentally, the proband rolled over between 6-8 months of age, sat at 24 months, and began crawling and pulling to stand at 4.5 years of age. He continued to be non-verbal, using signs and an augmented communication device in the school setting.

On physical exam at 6 years of age, the proband’s weight was 16.2 kg (–2 SD), height 97cm (–4 SD), and OFC was 47.8cm (–3 SD). He was found to be grossly microcephalic with frontal bossing, bitemporal narrowing and prominence of the parietal areas of his skull. He also had prominent metopic suture and supraorbital ridges. He had widely set eyes with sparse hair and eyebrows, bilateral ptosis, flattened midface, broad nasal root, normally formed philtrum and a slightly tented upper lip. Ears were slightly posteriorly rotated with prominent lobes. His upper dentition appeared normal. He had bilateral ptosis, (left greater than right) with exotropia. Hands showed bilateral clinodactyly, proximally placed thumbs, and tapering of his fingers. Feet showed overlap of his great and third toes over the second toe.

Subject 12 (M060721; p.Glu171Lys)

The male proband is the first child to healthy unrelated parents, with a younger healthy brother. At birth, the mother was 29 years old and the father 34 years old. The child was born by vaginal delivery at term following an uneventful pregnancy. Birth weight was 3170 grams (–1.5 SD), length 50 cm (0 SD), and OFC 34 cm (–1 SD). Apgar scores were 8 and 9 at 1 and 5 minutes, respectively. He was first evaluated by genetics at the age of 7 years. Weight was 26 kg (75^{th}-90^{th} centile), height 118 cm (25^{th}-50^{th} centile), OFC 50 cm (10^{th} centile). Physical examination showed microdolicocephalic skull, curly hair, bi-temporal constriction with mild prominence of the metopic suture, sparse hair and eyebrows, bilateral ptosis (more pronounced on the right), hypertelorism, epicanthal folds, flat nasal bridge, anteverted nares, prominent deeply grooved philtrum, low-set and posteriorly angulated ears with thickened helices, short webbed neck with pterygium coli and low posterior hairline, pectus deformity, dark skin, multiple cutaneous nevi. Developmental milestones were in the normal range. The child sat at age 7 months, and walked alone at age 13 months. Language was mildly delayed and learning difficulties were identified. The subject underwent surgical intervention for bilateral palpebral ptosis at 4 years of age. He also underwent surgical repair of right cryptorchidism at age 10 years. Brain MRI, two-dimensional color-Doppler echocardiography, renal ultrasonography, audiometric evaluation, and electroencephalogram were all normal.

The subject is now 12 years old. His weight is 44 kg (75^{th}-90^{th} centile), height 145 cm (25^{th}-50^{th} centile), and OFC 51.5 cm (3^{rd}-10^{th} percentile). Psychometric evaluation using the Leiter scale documented an intelligence quotient (IQ) of 91. Learning difficulties, particularly in reading and mathematics, problems in the field of visual/perceptual abilities-organizational skills, and attention deficit were documented. Previously performed genetic tests include array CGH, as well as sequencing of the *PTPN11*, *SOS1*, *SOS2*, *RAF1*, *KRAS*, *BRAF*, *MEK1*, *MEK2*, *NRAS*, and *SHOC2* genes, which were all normal.

Subject 13-15 (Pat30153, Fat30153 and Aunt30153; Family 30153; p.Glu171Lys)

The proband is a female with a history of pectus deformity, pulmonary stenosis, ptosis requiring surgery, optic atrophy and broad neck with a webbed appearance. She had several dysmorphic facial features including a broad forehead, hypertelorism, bilateral ptosis, and upturned and broad nasal tip, long philtrum, and low-set ears. Her adult height was 144 cm ($<3^{rd}$ percentile). Her mother (who was identified to not carry the *CDC42* mutation) was also short (147 cm, $<3^{rd}$ percentile), suggesting a familial contribution to her short stature. Her mutation-positive father has a history of a pectus deformity as well as several similar dysmorphic facial features. His adult height was 167 cm. Her mutation-positive paternal aunt has short stature (154 cm) and pectus deformity. She is reported to have a similar built and facial gestalt as the other affected family members, but she has never been evaluated personally by one of the authors. She has myocardial insufficiency and cardiac rhythm disturbance requiring implantation of a pacemaker device. It is not clear whether her cardiac problems have resulted from a congenital heart abnormality. She was diagnosed with glaucoma leading to loss of vision on the right eye. A cataract was removed at the age of 58 years. The paternal uncle also has a history of a pectus deformity, his height is 165 cm, and shared some of the same dysmorphic facial features. He has a son who also has dysmorphic facial features. For both of them, DNA was not available for molecular analysis. Similar clinical features were observed in the molecularly confirmed affected aunt The grandfather is predicted to have the mutation, but this has not been molecularly confirmed. He has a history of a ptosis, pectus deformity as well, and his adult height was 155 cm. The family tree is shown in Figure S1.

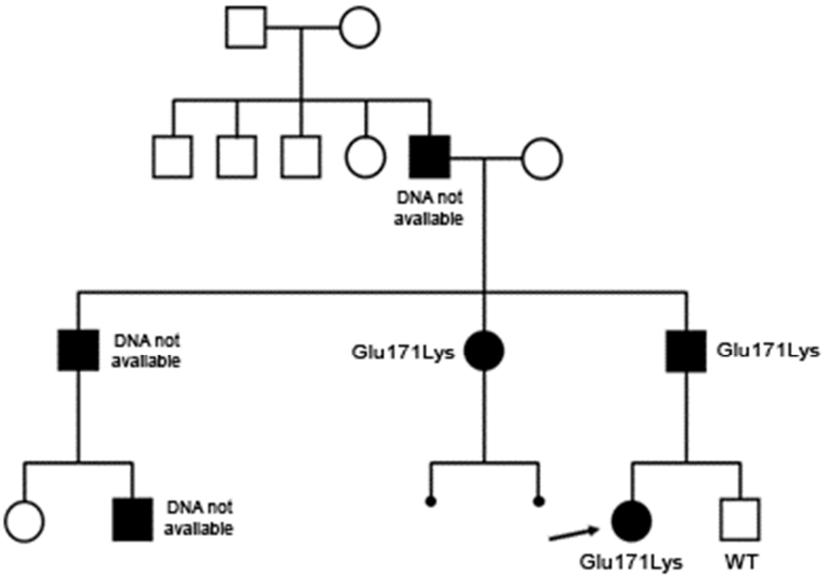

Figure S1. Pedigree of family 30153 showing transmission of the *CDC42* variant and its co-segregation with the trait. The affected index individual (subject 13) is indicated (arrow), together with the other genotypized members of the family, including her affected father and aunt (subjects 14 and 15), all of whom harbored the *CDC42* mutation (p.Glu171Lys). Three additional members of the family were clinically affected but DNA specimens were not available for mutation analysis.

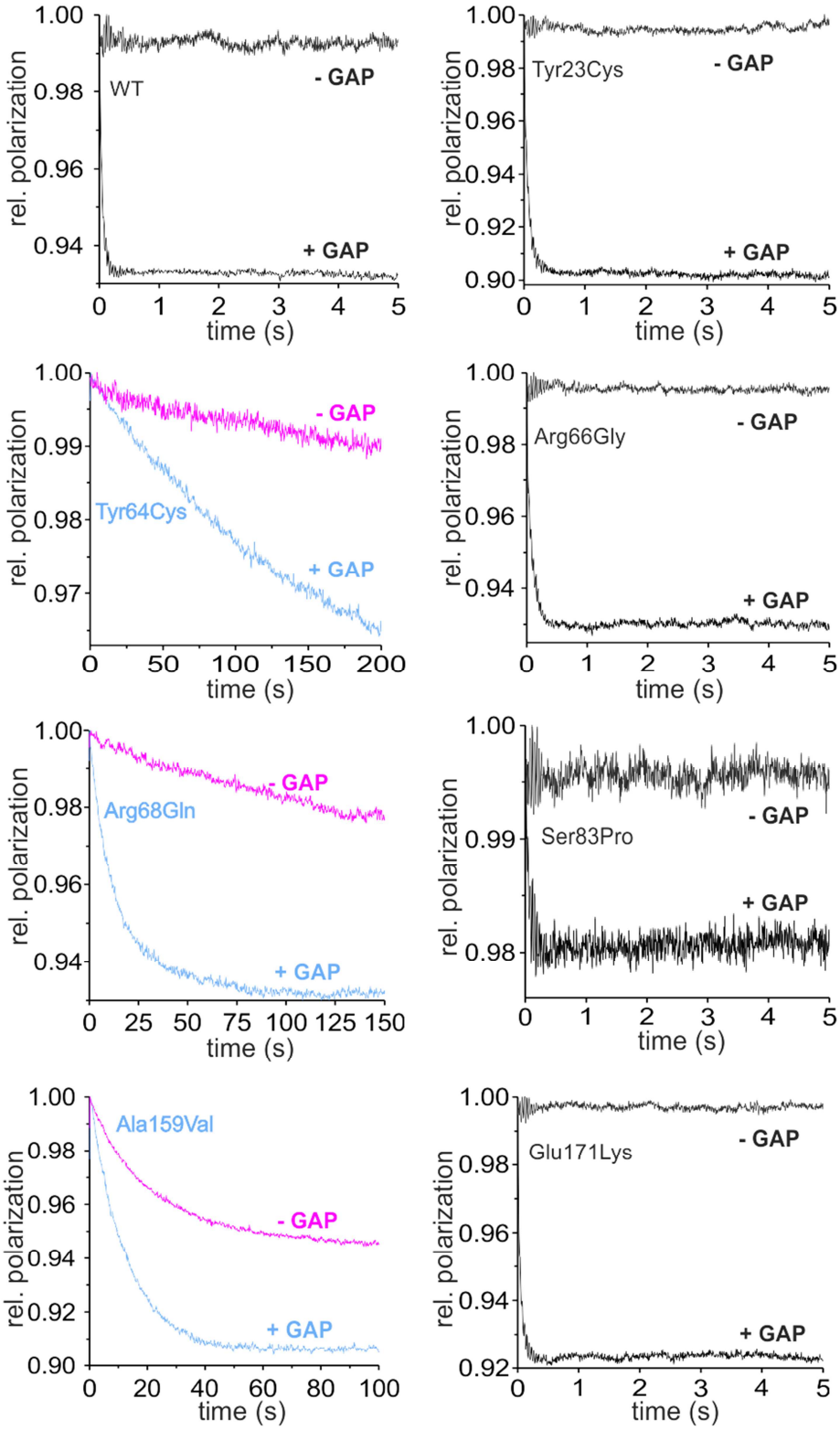

Figure S2. Basal and GAP-stimulated GTPase activity of disease-causing CDC42 mutants. Hydrolysis of tamraGTP was measured basally and following stimulation with ARHGAP1 ($p50^{GAP}$) in a stopped-flow machine. Although the $CDC42^{Tyr64Cys}$, $CDC42^{Arg68Gln}$ and $CDC42^{Ala159Val}$ mutants exhibited a slight ($CDC42^{Tyr64Cys}$, $CDC42^{Arg68Gln}$) or strong ($CDC42^{Ala159Val}$) increase in intrinsic GTP hydrolysis (magenta curves), they showed robust $p50^{GAP}$ insensitivity (blue curves). The data are represented as bar charts in **Figure 2A**.

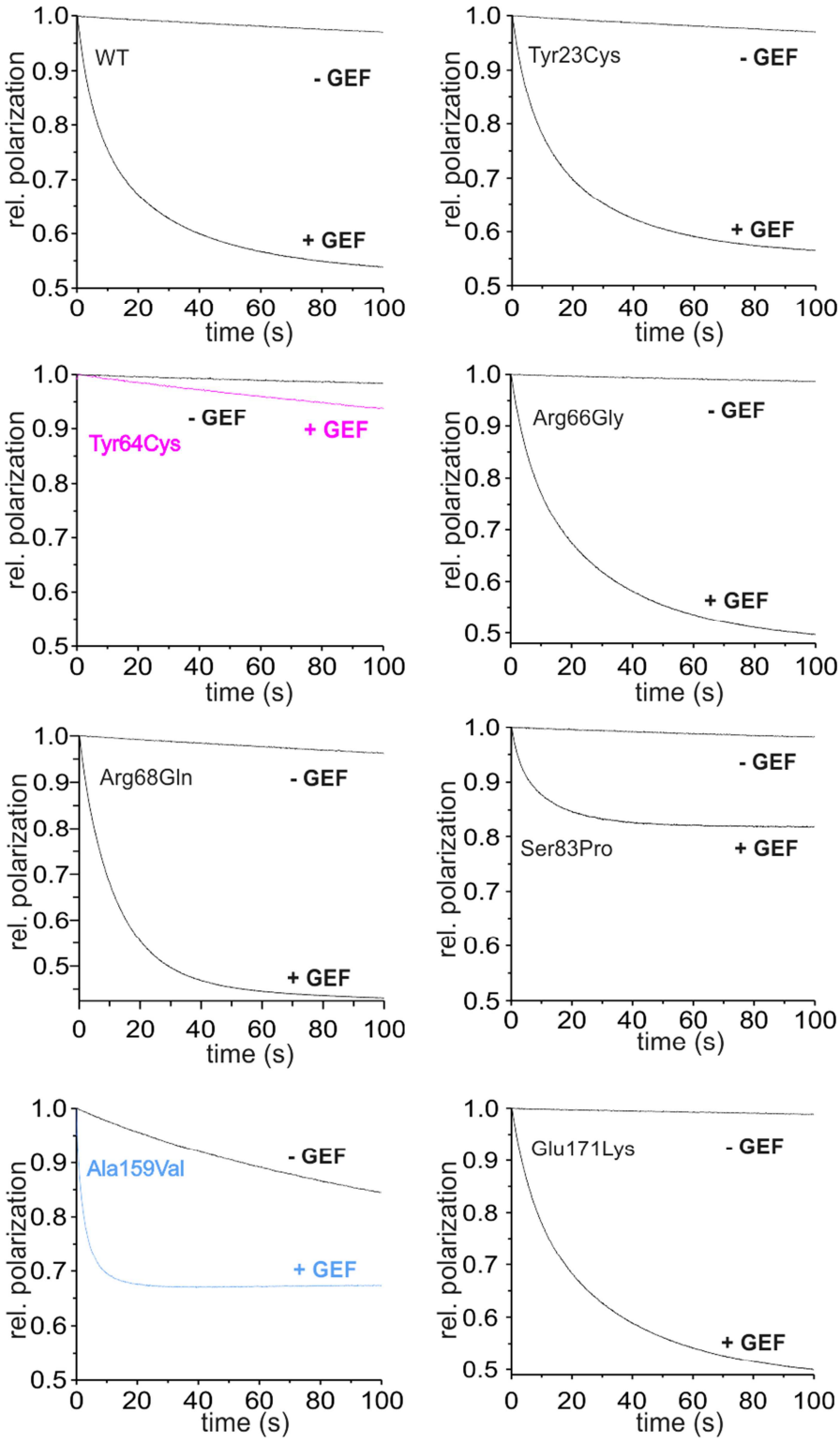

Figure S3. Basal and GEF-catalyzed nucleotide exchange reactions of disease-causing CDC42 mutants. The release of a fluorescently labelled GDP (mantGDP) was measured basally and with the catalytic domain of intersectin (ITSN1) in a stopped-flow machine. The CDC42^{Ala159Val} mutant exhibited a significantly increased intrinsic and GEF-catalyzed nucleotide release, while ITSN1 activity towards CDC42^{Tyr64Cys} was almost completely abolished (magenta curve). The data are represented as bar charts in **Figure 2B**.

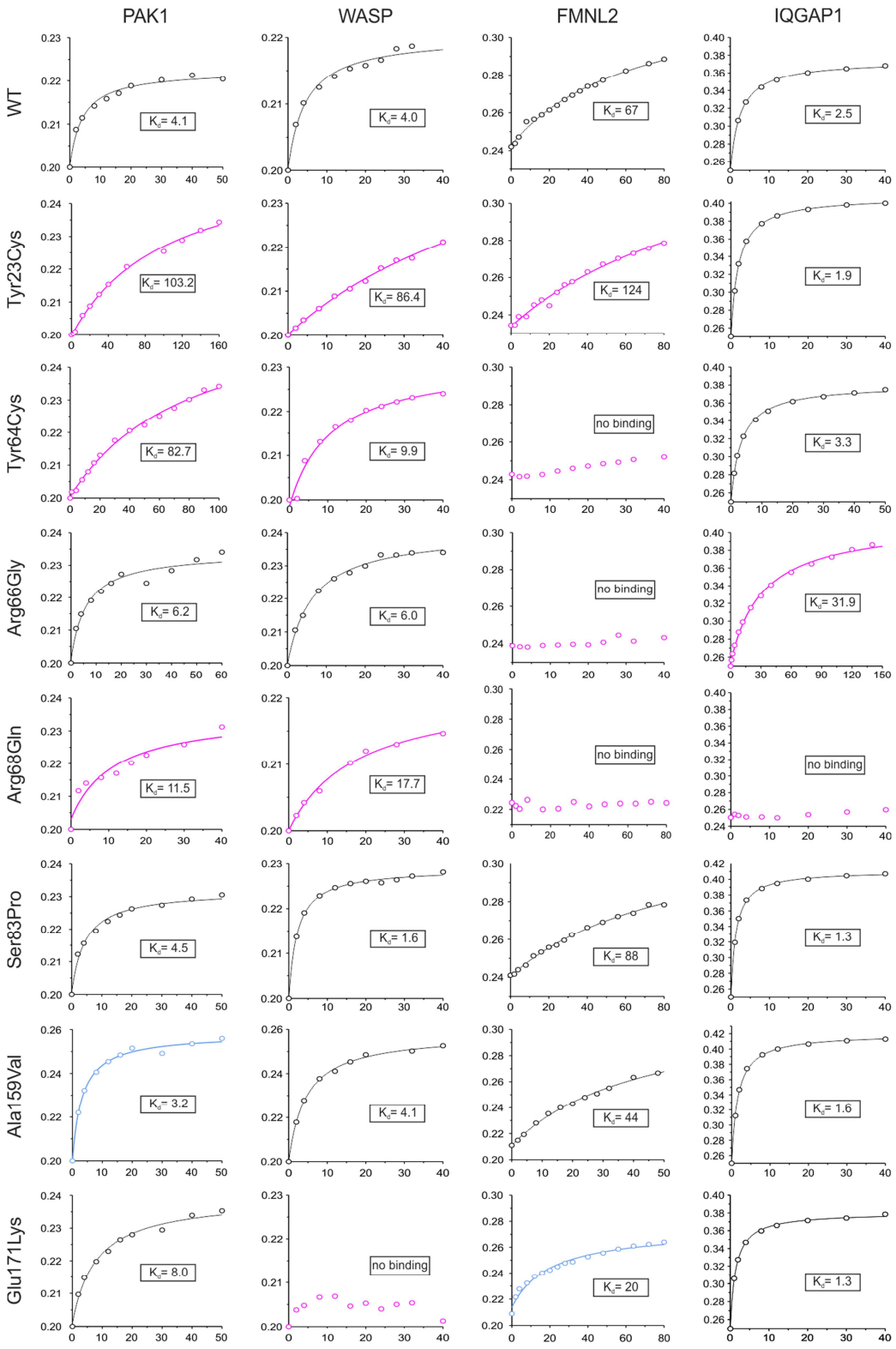

Figure S4. Binding of disease-causing CDC42 mutants to diverse effectors. Fluorescence polarization experiments were conducted to determine the dissociation constants (K_d) by titrating mantGppNHp-bound, active CDC42 variants with increasing concentrations of GTPase binding domains (GBD) of PAK1, WAS (WASP), FMNL2 and IQGAP1, as indicated. The y-axis represents fluorescence polarization, and the x-axis the concentration of the respective effector proteins as GST-fusion proteins in µM. Blue curves indicate increased binding affinity, whereas decrease or loss of binding is colored in magenta. Data are represented as bar charts in **Figure 2C**.

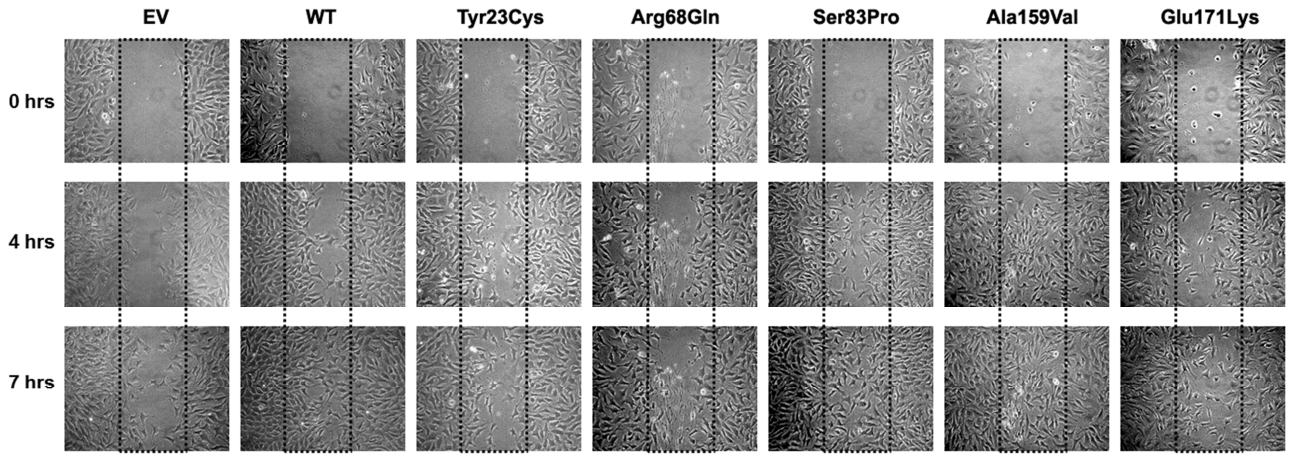

Figure S5. *CDC42* mutations differentially impact polarized migration. Wound-healing was performed using NIH3T3 cells transiently transfected to express wild-type CDC42 (WT), each of the $CDC42^{Tyr23Cys}$, $CDC42^{Arg68Gln}$, $CDC42^{Ser83Pro}$, $CDC42^{Ala159Val}$ and $CDC42^{Glu171Lys}$ mutants, or the relative empty vector (EV). A representative assay of three performed is shown. The wound was generated 24 hours after transfection, and migration in the wounded area was evaluated after, 0, 4 and 7 hours. Cells expressing exogenous wild-type CDC42 were shown to migrate more rapidly into the scratched area than cells transfected with the empty vector. Mutants were shown to differentially perturb polarized migration. Specifically, $CDC42^{Ser83Pro}$ and $CDC42^{Ala159Val}$ overexpression variably enhanced the wound closure ability of transfected cells compared to the wild-type protein, whereas expression of $CDC42^{Tyr23Cys}$, $CDC42^{Arg68Gln}$ and $CDC42^{Glu171Lys}$ failed to do that, supporting a gain-of-function and a loss-of-function effect of these mutants, respectively. Data are represented as bar charts in **Figure 3A**.

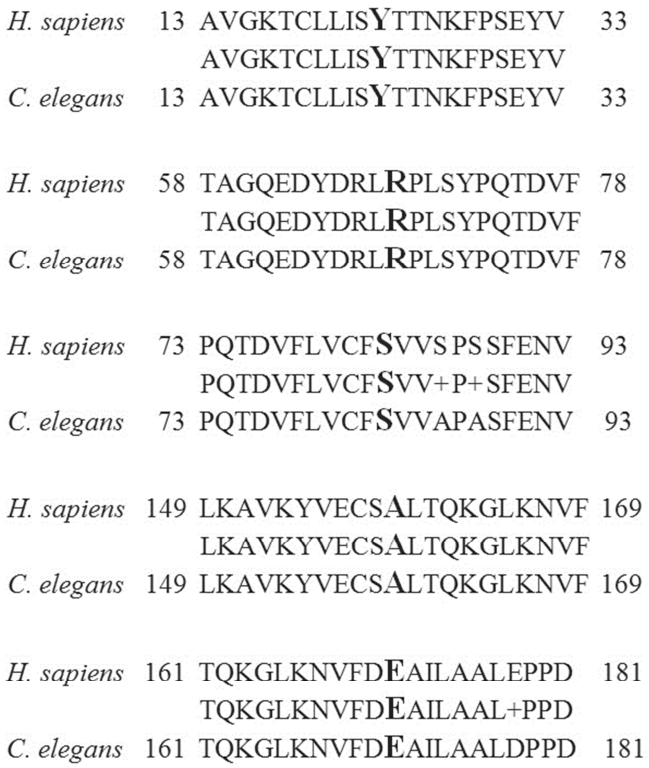

Figure S6. Amino acid sequence alignments of human CDC42 and the *C. elegans* ortholog. Stretches encompassing residues Tyr[23], Arg[68], Ser[83], Ala[159] and Glu[171] are shown, with affected residues shown in bold. Identity and conservation (+) of individual residues is also reported (middle row).

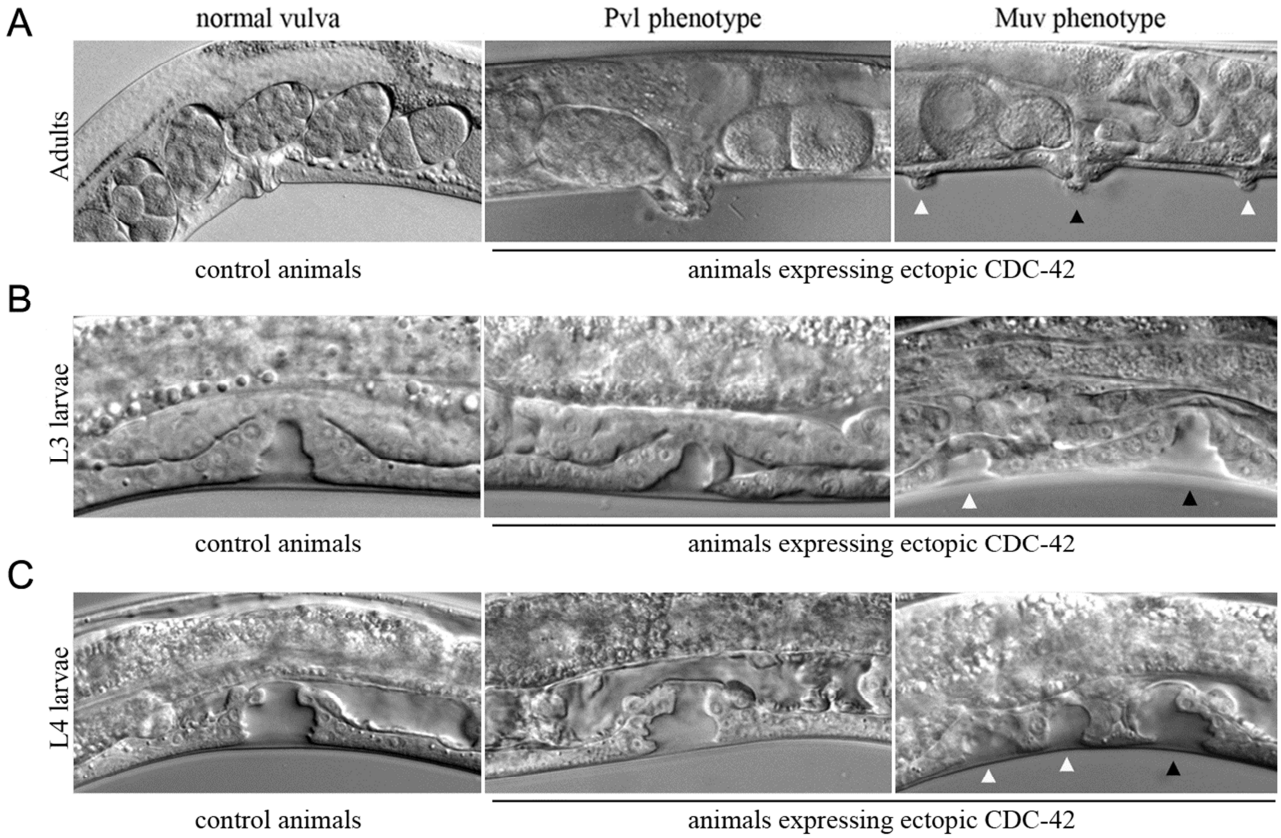

Figure S7. Consequences of *CDC-42* expression on vulval development in *C. elegans*. Ectopic expression of wild-type CDC-42 at the late L2/early L3 larval stages elicits multivulva (Muv) and protruding vulva (Pvl) phenotypes. Nomarski images show that a normal vulva develops in adult control animals (left), whereas a single protruding vulva (middle) or multiple ectopic pseudovulvae (right) are observed in a variable proportion of CDC-42-expressing animals (**A**). Black and white arrowheads point to the vulva and ectopic pseudovulvae, respectively. Nomarski images of vulval precursor cells (VPCs) at late L3 (**B**) and mid L4 (**C**) larval stages. In control animals, only P6.p descendants detach from the cuticle generating a single, symmetric invagination (left), whereas in CDC-42 expressing animals, VPCs descendants generates asymmetric invaginations (middle), or additional VPCs assume fate 1, generating multiple invaginations (right). Black and white arrowheads point to P6.p descendants-derived invagination and extra invaginations, respectively. Anterior is to the left and dorsal is up, in all images.

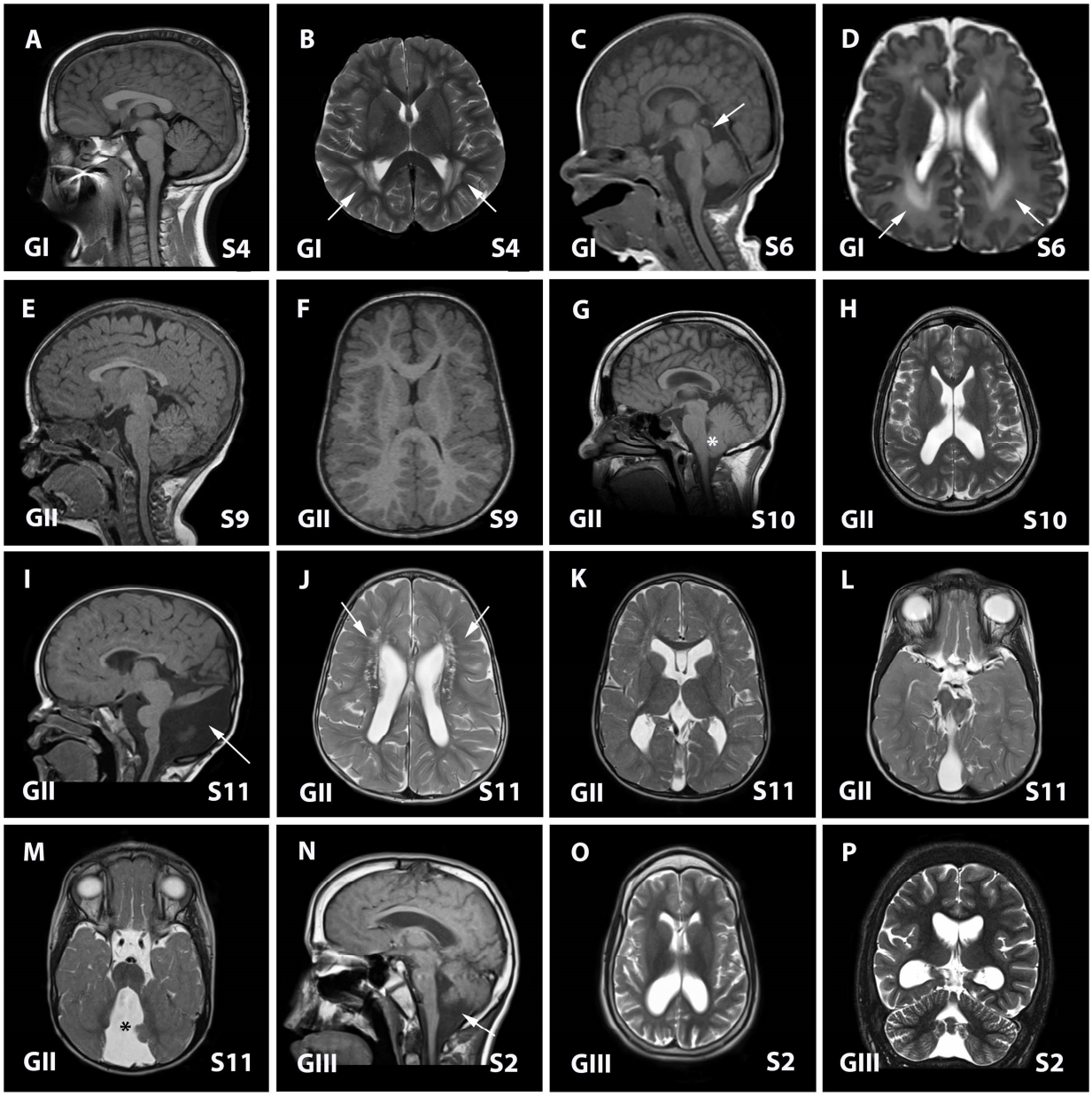

Figure S8. Brain MRIs of *CDC42* mutation-positive individuals. (**A-B**) Subject 4 (S4, p.Arg66Gly), T1-weighted mid-sagittal and T2-weighted axial images showing a thick corpus callosum, and white matter signal intensities in the posterior periventricular regions (arrows). (**C-D**) Subject 6 (S6, p.Arg68Gln), T1-weighted midsagittal and T2-weight axial images showing a thin corpus callosum, large tectum (arrow), mild ventriculomegaly, and white matter signal intensities in the posterior periventricular regions (arrows). (**E-F**) Subject 9 (S9, p.Ser83Pro), T1-weighted mid-sagittal and axial images showing a thin corpus callosum and deep cortical infolding (**G-H**) Subject 10 (S10, p.Ser83Pro), T1-weighted midsagittal and T2-weighted axial images showing mild cerebellar tonsillar ectopia (asterisk) and mild ventriculomegaly. (**I-M**) Subject 11 (S11, p.Ala159Val), T1-weighted para-sagittal and T2-weighted axial and coronal images showing a small and upward rotated cerebellar vermis consistent with a Dandy-Walker malformation (arrow, I; asterisk, M), thin corpus callosum, globular pons, white matter signal intensities in the frontal periventricular regions (arrows), mild ventriculomegaly, and asymmetric midbrain with a possible cleft in the tectum. (**N-P**) Subject 2 (S2, p.Tyr23Cys), T1-weighted para-sagittal and T2-weighted axial and coronal images showing a small and dysplastic cerebellar vermis (arrow, N), cerebral and cerebellar atrophy, and ventriculomegaly. Mutation groups (GI to GIII) are indicated.

Table S1. WES data output of *CDC42* mutation-positive individuals.

ID	WES enrichment kit	Sequencing platform	Target regions covered >10x	Target regions covered >20x	Average depth on target
Subject 1 (LR16-483)	SureSelect Clinical Research Exome	Illumina HiSeq2000	98.2%	96.4%	159x
Subject 2 (LR14-224)	SureSelect Human All Exon v1	Illumina HiSeq2000	91.2%	86.6%	110x
Subject 3 (LR17-420)	Nextera Exome Enrichment Kit	Illumina HiSeq2000	99.5%	99.0%	188x
Subject 4 (LR14-352)	SeqCap EZ VCRome 2.0	Illumina HiSeq2000	97.1%	94.3%	121x
Subject 5 (PCGC 1-04248)	SureSelect Human All Exon v5	Illumina HiSeq2000	98.3%	85.2%	82x
Subject 8 (LR17-032)	SureSelect Clinical Research Exome	Illumina HiSeq2000	97.0%	94.5%	104x
Subject 9 (LR10-046)	SeqCap EZ MedExome v2	Illumina HiSeq2000	89%	79%	57.2x
Subject 10 (LR16-056)	SureSelect Human All Exon v3	Illumina HiSeq2000	97.1%	85.3%	83.8x
Subject 11 (LR15-338)	SeqCap EZ MedExome v2	Illumina HiSeq2000	90%	80%	110x

Table S2. Interpretation of the identified *CDC42* variants according to ACMG criteria.

Amino acid change	Combining criteria for pathogenicity	ACMG codes	Specific criteria	ACMG classification
p.Ile21Thr	1 Strong, 2 Moderate and ≥2 Supporting	PS2; PM1, PM2; PP2, PP3	*de novo*; affecting a functional domain, absent in public databases; missense variant, variant predicted to be pathogenic	Pathogenic
p.Tyr23Cys	≥2 Strong	PS2, PS3	*de novo*; *in vitro*/*in vivo* functional studies documenting impact on protein function	Pathogenic
p.Tyr64Cys	≥2 Strong	PS1, PS2, PS3	known pathogenic variant; *de novo*; *in vitro* functional studies documenting impact on protein function	Pathogenic
p.Arg66Gly	≥2 Strong	PS2, PS3	*de novo*; *in vitro* functional studies documenting impact on protein function	Pathogenic
p.Arg68Gln	≥2 Strong	PS2, PS3	*de novo*; *in vitro*/*in vivo* functional studies documenting impact on protein function	Pathogenic
p.Cys81Phe	1 Strong, 2 Moderate and ≥2 Supporting	PS2; PM1, PM2; PP2, PP3	*de novo*; affecting a functional domain; absent in public databases; missense variant; predicted to be pathogenic	Pathogenic
p.Ser83Pro	≥2 Strong	PS2, PS3	*de novo*; *in vitro*/*in vivo* functional studies documenting impact on protein function	Pathogenic
p.Ala159Val	≥2 Strong	PS2, PS3	*de novo*; *in vitro*/*in vivo* functional studies documenting impact on protein function	Pathogenic
p.Glu171Lys	≥2 Strong	PS2, PS3	*de novo*; *in vitro*/*in vivo* functional studies documenting impact on protein function	Pathogenic

PS, pathogenic strong; PM, pathogenic moderate; PP, pathogenic supporting.
PS1: same amino acid change as a previously established pathogenic variant regardless of nucleotide change.
PS2: *de novo* (both maternity and paternity confirmed) in an affected subject with the disease and no family history.
PS3: well-established *in vitro* or *in vivo* functional studies supportive of a damaging effect on the gene or gene product.
PM1: located in a mutational hot spot and/or critical and well-established functional domain without benign variation.
PM2: absent from controls (or at extremely low frequency if recessive) in Exome Sequencing Project, 1000 Genomes or ExAC.
PP2: missense variant in a gene that has a low rate of benign missense variation and where missense variants are a common mechanism of disease.
PP3: multiple lines of computational evidence support a deleterious effect on the gene or gene product (e.g., conservation, evolutionary, splicing impact).

Table S3. Vulval phenotypes in nematodes expressing wild-type CDC-42 or the disease-associated mutants.

Genotype	Transgene	Pvl (%)	Muv (%)	Vul (%)	N
wild-type	-	0.5	0	0	>2000
wild-type	empty vector	0.9	0	0	233
wild-type	*cdc-42*^{WT}	18.3[a]	2.3[d]	0	1447
wild-type	*cdc-42*^{Tyr23Cys}	8.1[a,b]	2.9[d]	0	588
wild-type	*cdc-42*^{Arg68Gln}	12.6[a,c]	2.0[d]	0	810
wild-type	*cdc-42*^{Ser83Pro}	31.0[a,b]	4.5[d,c]	0	749
wild-type	*cdc-42*^{Ala159Val}	34.3[a,b]	5.8[d,e]	0	572
wild-type	*cdc-42*^{Glu171Lys}	8.5[a,b]	2.1[d]	0	943
let-60(n1046)	-	na	72.5	0	501
let-60(n1046)	*cdc-42*^{WT}	na	89.2[f]	0	182
let-23(sy1)	-	0	0	80.2	956
let-23(sy1)	*cdc-42*^{WT}	0	0	47.4[g]	475
let-23(sy1)	*cdc-42*^{Tyr23Cys}	0	0	47.5[g]	133
let-23(sy1)	*cdc-42*^{Arg68Gln}	0	0	47.8[g]	251
let-23(sy1)	*cdc-42*^{Ser83Pro}	0	0	30.2[g,h]	374
let-23(sy1)	*cdc-42*^{Ala159Val}	0	0	21.6[g,h]	236
let-23(sy1)	*cdc-42*^{Glu171Lys}	0	0	49.4[g]	166

Strains: *let-60(n1046)* is a gain-of-function allele of *let-60/RAS*; *let-23(sy1)* is a hypomorphic allele of *let-23/EGFR*.

Wild-type and mutant *cdc-42* alleles were expressed under the control of the *hsp16.41* inducible promoter. Animals were grown at 20 °C and heat-shocked at late L2/early L3 stages. *N* indicates the number of animals scored. Multivulva (Muv), protruding vulva (Pvl) and vulvaless (Vul) phenotypes are expressed as percentage of adults with ectopic pseudovulvae, exhibiting a protruding vulva or lacking a vulva, respectively.

na: not ascertained.

In all comparisons, *P*-values were calculated using two-tailed Fisher's exact test.

[a]Significantly different from animals expressing the empty vector ($P < 0.00005$).

[b]Significantly different from animals expressing *cdc-42*^{WT} ($P < 0.0001$).

[c]Significantly different from animals expressing *cdc-42*^{WT} ($P < 0.05$).

[d]Significantly different from animals expressing the empty vector ($P < 0.05$).

[e]Significantly different from animals expressing *cdc-42*^{WT} ($P < 0.001$).

[f]Significantly different from *let-60(n1046)* animals ($P < 0.00001$).

[g]Significantly different from *let-23(sy1)* animals ($P < 10^{-12}$).

[h]Significantly different from *let-23(sy1)* animals expressing *cdc-42*^{WT} ($P < 0.0001$).

Table S4. Impact of *wsp-1*/*WASP* RNA-mediated interference on vulval phenotypes in *C. elegans*.

Genotype	Transgene	Gene Modulated by RNAi	Time of exposure to RNAi bacteria (hours)	Pvl (%)	Muv (%)	N
let-60(n1046)	-	*let-60*	0	na	73.2	205
			2	na	44.0[a]	150
			4	na	34.2[a]	117
			8	na	25.8[a]	120
wild-type	-	*wsp-1*	0	0.7	0	150
			8	1.3	0.2	829
wild-type	*cdc-42^{WT}*	*wsp-1*	0	21.4	2.4	627
			2	19.5	1.8	56
			4	13.5[b]	1.8	168
			8	11.7[c]	4.1	410
wild-type	*cdc-42^{Tyr23Cys}*	*wsp-1*	0	7.5	2.6	154
			2	8.0	2.5	122
			4	7.1	2.4	85
			8	6.8	2.8	72
wild-type	*cdc-42^{Arg68Gln}*	*wsp-1*	0	13.6	2.7	86
			2	14.1	2.0	105
			4	12.5	2.8	72
			8	9.8	3.2	96
wild-type	*cdc-42^{Ser83Pro}*	*wsp-1*	0	31.2	4.2	214
			2	30.0	3.8	78
			4	35.0	4.0	101
			8	42.0[b]	4.9	205
wild-type	*cdc-42^{Ala159Val}*	*wsp-1*	0	42.3	6.3	189
			2	45.0	6.3	79
			4	48.0	5.9	119
			8	49.3	7.7	143
wild-type	*cdc-42^{Glu171Lys}*	*wsp-1*	0	8.7	2.3	263
			2	8.8	1.9	54
			4	8.3	2.2	89
			8	9.4	1.6	124

Synchronized adult hermaphrodites were left on agar plates seeded with RNAi bacteria for the indicated time. Screening of the protruding vulva (Pvl) and multivulva (Muv) phenotypes was carried out on F1 animals grown at 20 °C and heat-shocked at early L3 larval stage. *N* indicates the number of animals scored. As a control of the efficiency of the RNAi protocol, *let-60* RNAi was performed on animals carrying the activating p.Gly13Glu substitution in LET-60, which is associated with a high penetrant Muv phenotype.

wsp-1 RNAi had no vulva phenotype *per se*, but was shown to significantly reduce the prevalence of Pvl associated with expression of CDC-42^{WT} ($P < 0.0001$), indicating that occurrence of this phenotype is mediated, in part, by WSP-1. In contrast, the vulval defect observed in CDC-42^{Tyr23Cys}, CDC-42^{Arg68Gln} and CDC-42^{Glu171Lys} animals was not modulated by *wsp-1* RNAi, which is consistent with the collected biochemical data indicating abolished (CDC-42^{Glu171Lys}) or strongly reduced (CDC-42^{Tyr23Cys} and CDC-42^{Arg68Gln}) association of these mutants with WASP. The Muv phenotype was not modulated by *wsp-1* RNAi. *P*-values were calculated using two-tailed Fisher's exact test; na, not ascertained.

[a]Significantly different from non-interfered *let-60(n1046)* animals ($P < 0.0001$).

[b]Significantly different from the corresponding non-interfered animals ($P < 0.05$).

[c]Significantly different from the corresponding non-interfered animals ($P < 0.0001$).

Table S5. Clinical features of *CDC42* mutation-positive individuals.

Subject	1	2	3	4	5	6	7	8	9	10	11	12	13	14	15
ID	**LR16-483**	**LR14-224**	**LR17-420**	**LR14-352**	**PCGC 1-04248**	**ISS3MO**	**ISS4BO**	**LR17-032**	**LR10-046**	**LR16-056**	**LR15-338**	**M060721**	**Pat30153**	**Fat30153**	**Aunt30153**
Mutation group	**III**	**III**	**I**	**I**	**I**	**I**	**I**	**II**	**II**	**II**	**II**	**III**	**III**	**III**	**III**
Mutation	**p.I21T**	**p.Y23C**	**p.Y64C**	**p.R66G**	**p.R66G**	**p.R68Q**	**p.R68Q**	**p.C81F**	**p.S83P**	**p.S83P**	**p.A159V**	**p.E171K**	**p.E171K**	**p.E171K**	**p.E171K**
Sex	M	M	F	M	F	M	F	M	M	M	M	M	F	M	F
Age last assessed	10y	14y	15y	18y	8m	4y	5y	4y	6y	34y	6y	12y	Adult	Adult	Adult
Growth															
Birth weight	–2 SD	–1.5 SD	-2 SD	–4 SD	ND	0 SD	0 SD	–1.5 SD	0 SD	–0.75 SD	–2 SD	–1 SD	+0.25 SD	ND	ND
Birth OFC	ND	–2 SD	–2.2 SD	ND	ND	–0.25 SD	+1.5 SD	ND	ND	0 SD	–3 SD	–1 SD	ND	ND	ND
Postnatal weight	ND	–1 SD	–0.9 SD	–5 SD	–5 SD	–2.4 SD	–1.3 SD	ND	–1.5 SD	+2 SD	–2 SD	+0.5 SD	–2.5 SD	–1.5 SD	ND
Postnatal OFC	–2 SD	–3.5 SD	–4.3 SD	–0.5 SD	–3.5 SD	–2 SD	+0.25 SD	–2.6	+2 SD	0 SD	–3 SD	–1.7 SD	–3.5 SD	ND	ND
Postnatal growth deficiency	+	+	+	+	+	+	–	+	+	+	+	–	+	–	+
Neurologic Abnormalities															
DD/ID	+, no IQ testing, ADHD	++	++	++	+	++	++	++	++	++	++	–	–	–	–
Seizures	–	+	–	–	ND	–	+, 4 febrile	–	+	+, myoclonic	–	–	–	–	–
Tone	H	H	H, C	H	ND	C	–	–	–	C	H/C	–	–	–	–
Endocrine Issues															
Low GH	ND	+	–	+	ND	–	–	–	+	–	–	–	–	–	–
Hypothyroidism	ND	–	+	–	ND	–	–	–	+	–	–	–	–	–	–
Immunodeficiency	ND	–	+	+	ND	–	–	–	–	–	–	–	–	–	–
Other system abnormalities															
Hands-feet	ND	CD	CD, distal arthrogryposis	S	–	–	Long thin fingers	–	–	S/CD	S/CD	–	–	–	–
Eye abnormalities	Myopia	OA	Pale ON	Hyperopia, ST, OA, thick corneas	ND	ST	Astigmatism	ST	ST	ST	ST, OMP	Myopia, ST	ST, OA	–	GL, CA

Table S5 (continued)

Subject	1	2	3	4	5	6	7	8	9	10	11	12	13	14	15
ID	**LR16-483**	**LR14-224**	**LR17-420**	**LR14-352**	**PCGC 1-04248**	**ISS3MO**	**ISS4BO**	**LR17-032**	**LR10-046**	**LR16-056**	**LR15-338**	**M060721**	**Pat30153**	**Fat30153**	**Aunt30153**
Mutation group	**III**	**III**	**I**	**I**	**I**	**I**	**I**	**II**	**II**	**II**	**II**	**III**	**III**	**III**	**III**
Mutation	**p.I21T**	**p.Y23C**	**p.Y64C**	**p.R66G**	**p.R66G**	**p.R68Q**	**p.R68Q**	**p.C81F**	**p.S83P**	**p.S83P**	**p.A159V**	**p.E171K**	**p.E171K**	**p.E171K**	**p.E171K**
Skin	Several CALs	–	exzema	Multiple nevi	–	Maculopapular cutaneous eruption	–	–	–	–	–	Multiple nevi	–	–	–
Pectus	ND	–	–	–	–	+	–	–	–	–	–	+	+	+	+
Scoliosis	+	+	+	+	–	–	–	–	+	–	–	–	–	–	–
Inguinal hernia	+	+	+	–	–	+	+, bilateral	–	–	+	–	–	–	–	–
Cardiac defects	ND	–	ASD/VSD/PDA	–	–	HCM	VSD/PFO	–	TAPVR coarctation	–	PFO	–	Pulmonary stenosis	–	MI
GU defects	Unilateral renal agenesis	–	Renal pelviectasis	Renal dysplasia	–	–	–	Penile webbing	–	–	Hypospadias	–	–	–	–
Lymphatic malformations	–	–	–	+ pericardial effusion	–	–	–	–	–	+ pericardial effusions/gut	–	–	–	–	–
Platelets Large/Low	ND	–/–	+/+	+/–	ND	–/+	+/+	–	–/–	+/–	ND	–	–	–	ND
Recurrent Infections	+, recurrent OM	–	+	+	–	+	+	+	+	+	–	–	–	–	–

Abbreviations: ADHD, attention-deficit hyperactivity disorder; CALs, café au lait spots; C, contractures; CA, cataract; CD, camptodactyly; DD, developmental delay; F, female; GL, glaucoma; H, hypotonia; HCM, hypertrophic cardiomyopathy; ID, intellectual disability; m, month; M, male; MI, myocardial insufficiency; MPV, mean platelet volume; ND, no data; OA optic atrophy; OFC, occipitofrontal circumference; OM, otitis media; OMP, oculomotor palsy; ON, optic nerves; PFO, patent foramen ovale; S, syndactyly; SD, standard deviations; ST, strabismus; TAPVR, total anomalous pulmonary venous return; VSD, ventricular septal defect; y, year.

Table S6. Details of the facial features of *CDC42* mutation-positive individuals.

Subject	1	2	3	4	5	6	7	8	9	10	11	12	13	14
ID	**LR16-483**	**LR14-224**	**LR17-420**	**LR14-352**	**PCGC 1-04248**	**ISS3MO**	**ISS4BO**	**LR17-032**	**LR10-046**	**LR16-056**	**LR15-338**	**M060721**	**Pat30153**	**Fat30153**
Mutation group	**III**	**III**	**I**	**I**	**I**	**I**	**I**	**II**	**II**	**II**	**II**	**III**	**III**	**III**
Mutation	**p.I21T**	**p.Y23C**	**p.Y64C**	**p.R66G**	**p.R66G**	**p.R68Q**	**p.R68Q**	**p.C81F**	**p.S83P**	**p.S83P**	**p.A159V**	**p.E171K**	**p.E171K**	**p.E171K**
Sex	M	M	F	M	F	M	F	M	M	M	M	M	F	M
Age last assessed	10y	14y	15y	16y	8m	4y	5y	4y	6y	34y	6y	12y	Adult	Adult
Hair	ND	–	W	W	–	S/W	S	–	W	S/W	S	S	ND	ND
Eyebrows	ND	–	MF	–	–	S	S	–	–	–	S	S	–	–
Forehead	P	–	Short	B	–	P	B/P	B/P	B/P	P	P	–	B	B
Hypertelorism	ND	–	+	–	–	+	+ (mild)	+	+	+	+	+	+	–
Wide PF	+	+	–	–	–	–	–	+	–	–	+	+	–	–
Everted LE	ND	–	–	–	–	–	–	–	–	–	–	+	–	ND
Epicanthal folds	ND	+	–	–	–	+	–	+	–	–	–	+	+	–
Ptosis	–	+, U	–	+, B	–	–	–	+, B	–	+, B	+, B	+, B	+, B	–
Nasal bridge	H/N	H	N	H/N	–	W	W	W	W	W	W	W	W	–
Flared nostrils	–	–	+	–	–	+	+	+	–	+	–	+	+	–
Nasal tip Up/Broad	Broad	Up	Broad	Broad	–	Broad	Broad	Broad	–	–	Broad	Broad	Up/ broad	Up/ broad
Low-hanging columella	–	+	++	–	–	–	–	–	–	–	–	–	–	–
Underdeveloped midface	+	–	+	–	–	+	+	+	–	–	+	–	–	–
Philtrum	–	Short	Short	–	–	Long	Long	Long	Long	–	–	Deep	Long	Long
Thin upper vermillion	–	–	++	+	–	+	+	+	+	–	–	+	+	+
Mouth	CD/W	CD	W	W	–	–	CB	+	CB/W	W	CB/W	–	CD	–
Ears	L	–	S, LS	–	–	TH	LS	LS	LS	–	–	L/LS	LS	LS
Other facial features	Synophrys, PMS	Long neck	UPF, MF, small chin	Cleft palate, WSP	–	Neck webbing	–	–	Broad jaw, WSP	Broad jaw, WSP	–	Neck webbing	Neck webbing	Neck webbing

Abbreviations (ordered by feature): Hair: sparse (S), whorls (W); Eyebrows: medial flared (MF), sparse (S); Forehead: broad (B), prominent (P); PF, palpebral fissures; LE, lateral eyelids; Ptosis: unilateral (U), bilateral (B); Nasal bridge: high (H), narrow (N), wide (W); Mouth: cupid bow (CB), corners down (CD), wide (W); Ears: large (L), low-set (LS), small (S), thick helix (TH); UPF, upslanting palpebral fissures; PMS, prominent metopic suture; WPS, widely spaced teeth.

Table S7. Neuroimaging features of *CDC42* mutation-positive individuals.

Subject	**1**	**2**	**3**	**4**	**6**	**7**	**8**	**9**	**10**	**11**
ID	**LR16-483**	**LR14-224**	**LR17-420**	**LR14-352**	**ISS3MO**	**ISS4BO**	**LR17-032**	**LR10-046**	**LR16-056**	**LR15-338**
Mutation group	**III**	**III**	**I**	**I**	**I**	**I**	**II**	**II**	**II**	**II**
Mutation	**p.I21T**	**p.Y23C**	**p.Y64C**	**p.R66G**	**p.R68Q**	**p.R68Q**	**p.C81F**	**p.S83P**	**p.S83P**	**p.A159V**
Age at scan	13m	12y	3y	ND	5m	ND	34y	3y	34y	3y
Cortex	–	Diffuse atrophy	–	–	–	SEH	–	–	–	–
White matter	–	Decreased	Mildly thin	Mildly prominent PV WM signal intensities (posteriorly)	Mildly prominent PV WM signal intensities (posteriorly)	-	–	Mild periventricular WM abnormalities (PVL)	–	WM signal intensities
Ventricles, extra-axial space	–	VMEG	VMEG	–	VMEG, increased extra-axial space	–	–	Hydrocephalus s/p shunting	VMEG	–
Corpus callosum	–	Thin	Thin	Mildly thick	Mildly thin	pACC	Mild pACC	Mildly thin	–	pACC
Cerebellum	–	Diffuse atrophy, mild vermis hypoplasia	–	–	–	–	Mega cisterna magna	–	CBTE	Large PF, cerebellar foliar dysplasia, large ICP, small MCP, stretched SCP, severe DWM
Basal ganglia/thalami	–	–	–	–	–	–	–	–	–	Dysplastic thalami
Brainstem	–	–	–	–	Large tectum	–	–	–	–	Small medulla/pons, cleft in the tectum, abnormal superior colliculi
Hippocampi	–	–	–	–	–	–	–	–	–	Unilateral HIP dysplasia

Abbreviations: pACC, partial agenesis of the corpus callosum; CBTE, cerebellar tonsillar ectopia; DWM, Dandy-Walker malformation; HIP, hippocampal dysplasia; ICP, inferior cerebellar peduncle; MCP, middle cerebellar peduncle; PF, posterior fossa; PV, perivascular; PVL, periventricular leukomalacia; SCP, superior cerebellar peduncle; SCV, small cerebellar vermis; SEH, subependymal heterotopia; VMEG, ventriculomegaly; WM, white matter.